Journal of Hydrology 675 (2026) 135619

Contents lists available at ScienceDirect

Journal of Hydrology

journal homepage: www.elsevier.com/locate/jhydrol

Research papers

Is the Weibull distribution reliable to describe the rainfall kinetic power and momentum in Mediterranean environments?

F.G. Carollo [a], R. Caruso [a], V. Ferro [a,b], M.A. Serio [a,*]

[a] Department of Agricultural, Food and Forest Sciences, University of Palermo, Viale delle Scienze, Building 4, 90128 Palermo, Italy
[b] NBFC, National Biodiversity Future Center, 90133 Palermo, Italy

ARTICLE INFO

This manuscript was handled by Marco Borga, Editor-in-Chief, with the assistance of Luca Mao, Associate Editor

Keywords:
Rainfall erosivity
Rainfall intensity
Raindrop size distribution
Kinetic power
Weibull distribution

ABSTRACT

Understanding the characteristics of the rainfall drop size distribution (DSD) at the land surface is crucial for elucidating the mechanisms of precipitation that affect soil erosion processes. This study aims to both apply the Weibull distribution to more than 47,000 DSDs detected at Palermo (Italy) and El Teularet (Spain) experimental sites and deduce theoretically relationships for estimating the rainfall kinetic power and momentum of a DSD distributed as Weibull law having known parameters. The study confirms that the theoretical Weibull distribution can accurately reproduce measured DSDs, with highly consistent fitting results using the moment method (MM) for estimating its parameters. The results indicate that rainfall kinetic power and momentum are closely related to the characteristics of the DSD. No statistically significant correlation between the parameters of the Weibull distribution and rainfall intensity is detected. Moreover, the analysis highlights that the η parameter turns out to be related to the coefficient of variation of the DSD, and the parameter N_0 represents the total number of drops, making the Weibull distribution physically based. Furthermore, a comparison between the Weibull and Ulbrich distributions allows for the conclusion that, although both models exhibit similar performance in terms of fitting and reliability when describing rainfall kinetic power and momentum, the Weibull distribution offers advantages related to parameter estimation. Specifically, its parameters, unlike those of Ulbrich, possess a physical, and not merely statistical, significance. The study concludes that the Weibull distribution is highly reliable for characterizing rainfall kinetic power and momentum in two experimental sites located in the Mediterranean region, and rainfall intensity cannot serve as a variable to comprehensively represent the characteristics of precipitation.

1. Introduction

In soil erosion processes precipitation plays a fundamental role in soil particle detachment and transport (Pampalone et al., 2023). The rainfall intensity and the rainfall depth are the most relevant and commonly used variables for a climatic characterization of an investigated area. Furthermore, the drop size distribution (DSD), which refers to the frequency distribution of drops reaching a unit horizontal area within a unit time, is also considered a suitable indicator for characterizing precipitation, particularly when the study of soil erosion effects is required (Waldvogel, 1974; Uijlenhoet and Stricker, 1999; Carollo et al., 2016a, b; Serio et al., 2019a).

During the years, measurements carried out in different climate contexts demonstrated that the rainfall intensity is not fully representative of the rainfall energy as other rainfall characteristics, that could be obtained by the DSD, play a role in rainfall erosivity (Parsons and Gadian, 2000; Salles et al., 2002; Carollo et al., 2016b; Carollo et al., 2018; Serio et al. 2019a, b).

Serio et al. (2019a) and Carollo et al. (2023) using DSD measurements performing in three sites, characterized by similar climatic and geographic conditions, and with the same optical disdrometer, tested the empirical relationship proposed by Wischmeier and Smith (1978) to estimate the rainfall kinetic power, i.e. kinetic energy referred to unit time and area, P_n, (J m^{-2}h^{-1}), that is the most widely used relationship for quantifying the rainfall erosivity in soil erosion models. This relationship, which was originally deduced using data recorded in Missouri, Iowa e Wisconsin (Laflen and Moldenhauer, 2003) and was positively tested in different sites in the United States (Wischmeier, 1959), has the following expression:

* Corresponding author.
E-mail address: mariaangela.serio@unipa.it (M.A. Serio).

https://doi.org/10.1016/j.jhydrol.2026.135619
Received 7 April 2025; Received in revised form 10 January 2026; Accepted 1 May 2026
Available online 2 May 2026

$$\frac{P_n}{I} = \begin{cases} (11.9 + 8.73 logI) for I < I_t \\ (11.9 + 8.73 logI_t) for I \geq I_t \end{cases} \quad (1)$$

in which I is the rainfall intensity (mm/h), I_t is the *intensity threshold value* that according to Wischmeier and Smith (1978) is equal to 76 mm/h. Eq. (1) establishes that the ratio P_n/I, which represents the kinetic power per unit volume of rainfall, increases for rainfall intensity value less than I_t while it becomes constant for rainfall intensity greater than or equal to I_t. Wischmeier and Smith (1978) justified this threshold value suggesting that the median volume diameter, D_0, which is the drop diameter that divides the DSD into two parts of equal volume, does not continue to increase when rainfall intensities exceed 76 mm/h. Some authors, i.e. Lim et al. (2015), Angulo-Martínez et al. (2016), Carollo et al. (2016b), carrying out an analysis on P_n by raindrop size distribution, DSD, detected in different climatic contests confirmed the existence of a site-specific rainfall intensity threshold value.

Carollo et al. (2023), considering DSDs detected in two Sicilian experimental sites (Palermo and Sparacia), demonstrated that for a fixed rainfall intensity, especially for $I < 100$ mm/h, both the DSDs and the values of rainfall kinetic power, P_n (J m^{-2}h^{-1}), are different, and that the P_n-I relation, as Eq. (1), is site dependent (Carollo et al., 2016a; Serio et al., 2019a, b). Furthermore, in agreement with Van Dijk et al. (2002), Salles et al. (2002), Meshesha et al. (2014), the applicability of the most used empirical P_n-I relationships to geographical regions different to those of their original deduction can be limited and often requires calibration based on specific datasets (Rosewell 1986; Angulo-Martínez et al., 2016; Serio et al. 2019a; Carollo et al., 2023). To date no device, enabling to a direct and accurate measurement of the rainfall kinetic energy exists. Some authors (Waldvogel, 1974; Uijlenhoet and Stricker, 1999; Cevasco et al., 2015; Meshesha et al., 2019; Carollo et al., 2023) stated that the *DSD* is more suitable for characterizing the precipitation when the soil erosion effects must be studied.

To date the DSD formation is not fully understood, because of the random and complex nature of the physical phenomena that govern the aggregation and disaggregation of the raindrops (Falkovich et al., 2002). Villermaux and Bossa (2009) stated that the rain reaching the ground is the product of rupture and coalescence phenomena between colliding drops and furtherly the result of the breakup of individual large drops. This last phenomenon comes from the rapid fragmentation of single large drops due to aerodynamic instability and surface tension.

The knowledge of DSD enables to (i) understand how the rainfall is constituted of different drop sizes, (ii) compute the rainfall kinetic power, P_n (J m^{-2}h^{-1}), and momentum, M (N m^{-2}), in addition to rainfall intensity, I (mm/h), to characterize the precipitation from an energetic point of view, and (iii) understand how soil sealing and erosion processes are affected by the climatic forcing (Mualem and Assouline, 1989).

Over the years, several analytical forms of raindrop size parameterization have been proposed, such as lognormal (Feingold and Levin, 1986), Weibull (Sekine and Lind, 1982), exponential (Marshall and Palmer, 1948), and gamma (Ulbrich, 1983) distributions. The comparison between these commonly used distributions was carried out only for meteorological studies (Abas et al., 2014; Assouline, 2020), for determining the risk, uncertainty and money loss (Tao et al., 2002) and the best-fit distribution for the annual rainfall data (Kumar and Jahangeer, 2017; Olivera and Heard, 2019). However, to the best of our knowledge, for meteorological and soil erosion purposes, the skewed gamma distribution is the theoretical probability law most widely applied to measured DSDs, although the statistical parameters of the probability distribution have no physical meaning (Khrgian et al. 1952; Levin, 1963; Sulakvelidze, 1969; Sulakvelidze and Dadali, 1971; Ulbrich, 1983; Uijlenhoet and Stricker, 1999, Tokay et al., 2001; Salles et al., 2002; Bringi et al., 2003; Zhang et al., 2003; Carollo and Ferro, 2015; Carollo et al., 2016a, b; Seela et al., 2018; Serio et al. 2019a; Carollo et al., 2023). The wide applicability of the gamma distribution is attributed to its high adaptability to measured DSDs, irrespective of the specific parameter estimation technique employed.

The Weibull distribution was for the first time introduced by the Swedish physicist Weibull (Weibull, 1951) and, over the years, has been applied in many different scientific fields (like material science, engineering, physics, meteorology, medicine, economics, and quality control) and a few times for describing the raindrop size distribution.

For meteorological purposes, Sekine and Lind (1982) proposed the Weibull distribution for the first time in the following form:

$$N(D)dD = N_0 \frac{\eta}{\sigma}\left(\frac{D}{\sigma}\right)^{\eta-1} exp\left[-\left(\frac{D}{\sigma}\right)^{\eta}\right] dD \quad (2)$$

in which $N(D)$ is the number of drops within the range $(D, D + dD)$, N_0 is a parameter which Sekine and Lind (1982) assumed constant and equal to 1000 m^{-3}, η is the dimensionless shape parameter, and σ (cm) is the scale parameter of the Weibull distribution. For η equal to 1, the Weibull distribution is identical to the exponential distribution proposed by Marshall and Palmer (1948) (Sekine and Lind, 1982); for η equal to 2, the Weibull distribution reduces to Rayleigh distribution (Cohen, 1965). In other words, the Weibull distribution has also the merit to accept as specific cases other theoretical probability distributions. Eq. (2) is the scientific basis of the theoretical analysis which will be developed in this study and presented in the Materials and Methods section of this paper.

Considering the raindrop size distributions detected by Laws and Parsons (1943), Sander (1975), and Wickerts (1982), Sekine and Lind (1982) found that both η and σ parameters are related to the rainfall intensity according to a power low relationship while N_0 is equal to 1000 m^{-3}, but these empirical results does not provide any information about the physical meaning of the Weibull distribution. Furthermore, this distribution presents a peak and shifts to large raindrop diameters with increasing rainfall intensity (Jiang et al., 1997).

Liu and Hallett (1998) stated that variations in thermodynamic and dynamic parameters, such as temperature and vertical velocity, induce fluctuations in cloud droplet size distributions (Ackerman, 1967; Baumgardner et al., 1993). This variability implies that such distributions are characterized by multiplicity rather than uniqueness of DSDs. Under the assumption of an ideal system with conserved mass, Liu and Hallett (1998) derived that the maximum likelihood distribution corresponds to a Weibull distribution.

To date, the Weibull distribution has been used and tested above all for meteorological purposes and scarcely for hydrological ones. For example, some Authors (Sekine et al., 1987; Sekine et al., 1988; Jiang et al., 1996, 1997; Kumar and Jahangeer, 2017) considered this distribution for microwave applications, such as rain attenuation, and for cases in which drizzle, widespread and shower rain occurred and for studying the extreme rainfall events (Olivera and Heard, 2019).

Jiang et al. (1997) carried out a comparison between the most used frequency distributions (i.e. exponential, gamma, and Weibull) using DSD measurements obtained in Tokyo. They concluded that the exponential distribution better fits the experimental data for low rainfall intensity values ($I = 1.88$ mm/h), instead, for high rainfall intensity values ($I > 20$ mm/h), the gamma (Ulbrich, 1983) and Weibull distributions give better agreement with experimental data than the exponential one.

Alonge and Afullo (2012), carrying out an analysis to estimate the Weibull parameters using the third, fourth, and sixth moments of the momentum method, positively tested the Weibull distribution using DSD data collected by an RD-80 disdrometer installed at the Durban area (South Africa). They stated that the accuracy of the fit, and thus of the Weibull parameters estimates, decreases as rainfall intensity increases, probably due to the low sample size.

Assouline and Mualem (1989), considering the Weibull distribution, suggested a new approach for studying the mechanism of the forces that shape the raindrop size distribution through coalescence and breakup processes along their pathway from the cloud to the soil surface. The Authors stated that the hypothesis of uniform random raindrop fragmentation yielded to consider the measured DSD identical to the Weibull distribution since the probability for a drop break up is proportional to its relative volume, i.e. the Weibull distribution has the merit to be physically based. Then they suggested a new probability distribution function, named "*universal distribution*", which is independent of both the rainfall intensity and the site where precipitation occurs (Assouline and Mualem, 1989). Assouline and Mualem (1989) and Assouline (2009) positively tested this approach using DSD measurements carried out in different experimental areas (Rhodesia by Hudson (1965); Baton Rouge and Holly Springs by Carter et al. (1974); Princeton (New Jersey) by Smith et al. (2009)).

More recently, Carollo and Ferro (2015), for the first time, theoretically deduced a relationship to estimate kinetic power (see below the paragraph 2.3 of the section "Materials and Methods) considering the raindrop size distribution proposed by Ulbrich (1983) and the terminal falling drop velocity $V(D)$ (m/s), estimated using the empirical relationship proposed by Ferro (2001), according to which for natural precipitation the terminal velocity depends only on the raindrop diameter.

According to the relationship of Carollo and Ferro (2015), the kinetic power per unit volume of rainfall is only a function of the shape and scale parameters of the Ulbrich distribution. Carollo et al. (2016b), Carollo et al. (2018), Serio et al. (2019a, b) and Carollo et al. (2023) using DSDs measurements carried out using the same optical disdrometer at Palermo (Italy), Sparacia (Italy) and El Teularet (Spain) experimental areas, at fist positively tested the Gamma distribution. Then P_n relationship, theoretically deduced by Ulbrich distribution, resulted to be reliable for having a good estimation of the rainfall kinetic power in the Mediterranean environment, concluding that for energetically characterizing the precipitation it is enough to know how the rainfall is made up.

To date, at the best of our knowledge, no closed-form equation to estimate P_n has been theoretically deduced by Weibull distribution, and only some theoretical distributions can be associated with a specific relationship for the estimation of the raindrop terminal velocity to obtain theoretical closed-form relationships to estimate P_n and M. Furthermore, for an investigated area the estimate of rainfall erosivity is often carried out by applying empirical relationships linking kinetic power P_n with rainfall intensity I, as Eq. (1) by Wischmeier and Smith (1978), (Van Dijk et al., 2002). From a practical standpoint, these empirical relationships are site-specific (Carollo et al., 2016a; Serio et al., 2019a, b), do not consider the variability of DSD with rainfall intensity and need to be recalibrated. In addition, currently, no devices are available to measure P_n/I directly. Therefore, to obtain accurate estimates of P_n/I, it is necessary to know the DSD and determine its distribution parameters.

In this paper, the reliability of the Weibull distribution to reproduce rainfall DSDs measured in two sites located in the Mediterranean basin is firstly presented. Then a theoretical analysis is carried out to prove that the Weibull law is a physically based distribution and to develop rainfall kinetic power and momentum relationships of a DSD distributed by this law. Finally, disdrometric measurements of raindrop size distribution are used to fitting of Weibull and Ulbrich distributions and their reliability for describing rainfall kinetic power and momentum.

2. Materials and methods

2.1. Experimental sites and raindrop size distribution measurements

Drop size distribution measurements were carried out using the same optical disdrometer placed, in different periods, at the Palermo, and El Teularet experimental areas (Fig. 1). In particular, the former is located at the Department of Agricultural, Food and Forest Sciences of the University of Palermo, at 40 m a.s.l. (Fig. 1a), with a Mediterranean temperate climate (Köppen's Csa type), characterized by dry and hot summer and mild and rainy winter. The average annual temperatures range between 15 °C and 22 °C, while rainfalls, mainly concentrated in autumn and winter, show mean annual value of 654 mm. El Teularet experimental site is located at Sierra de Enguera, 100 km southwest of Valencia, at 760 m a.s.l. (Fig. 1b). Climate is Typical Mediterranean with 3–5 months of summer drought, usually from late June to September. Mean annual rainfall at the study area range from 479 mm at the Enguera-Las Arenas meteorological station to 590 mm at the Enguera Confederación Hidrográfica del Jucar (CHJ) meteorological station. Rainfall is distributed homogenously among spring, autumn and winter, while the summer is extremely dry due to high temperatures and lack of rainfall (García-Orenes et al., 2009). Mean annual temperature ranges from 12.7 °C at the Enguera-Las Arenas meteorological station to 14.2 °C at the Enguera Confederación Hidrográfica del Jucar (CH) meteorological station (García-Orenes et al., 2009).

Further details on these experimental installations are reported in previous papers (Bagarello and Ferro, 1998; Bagarello et al., 2013; Carollo et al., 2018). The two investigated locations are fully representative of Mediterranean climatic conditions, and the time span of collected measurements is long enough to cover rainfall events occurring under different climatic conditions and representative of severe soil erosion processes.

For each rainy minute, the optical disdrometer (model ODM 470 made by Eigenbrodt) (Fig. 2) measured drop diameters in the range of 0.05–0.6 cm. Each drop was separately measured and registered into classes of about 0.005 cm in width. The disdrometer divides the diameter range into 128 classes and gives the number of drops belonging to a particular class for each recording minute. The disdrometer measures, at

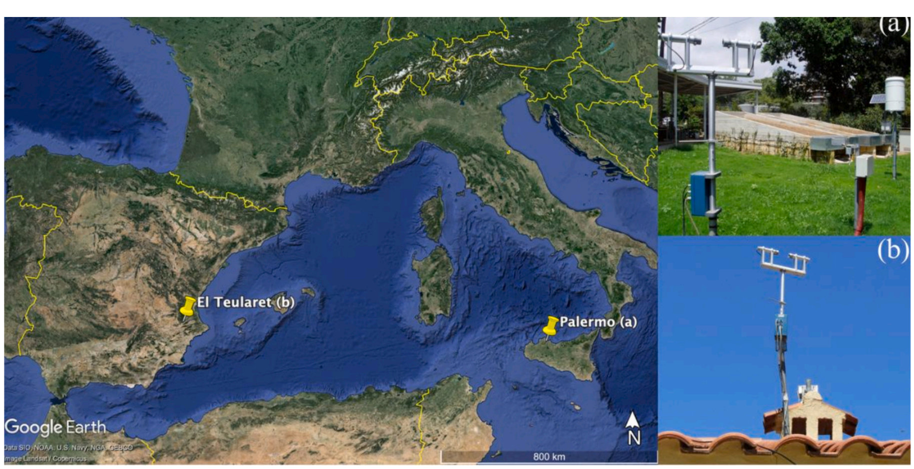

Fig. 1. View of Palermo (a) and El Teularet (b) experimental stations.

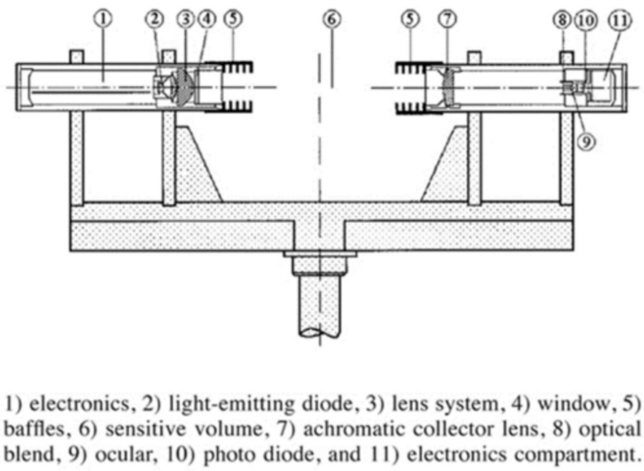

Fig. 2. Vertical section of the optical disdrometer (model ODM 470 made by Eigenbrodt).

1-minute time intervals, the number of drops in each class and the corresponding rainfall intensity. Grossklaus et al. (1998) proves that the disdrometer tends to underestimate the concentration of small droplets due to aerodynamic effects and the specific constraints related to the purposes for which it is designed (i.e., shipborne installation under high-wind conditions). Small droplets, characterized by low inertia, tend to follow the streamlines of the airflow around the instrument housing, thereby bypassing the sensitive volume (Grossklaus et al., 1998). Additionally, mechanical vibrations inherent to shipboard operations can generate electronic noise signals that mimic the signature of small droplets. Consequently, to prevent false positives, the instrument is configured to discard signals corresponding to droplets smaller than 0.4 mm (Grossklaus et al., 1998). Moreover, the disdrometer does not account for the oblateness of large hydrometeors, leading to a slight underestimation of the drop volume (Lempio et al., 2007).

Further details on the DSD measuring technique are reported in previous papers (Carollo et al., 2016a; Carollo et al., 2018; Serio et al., 2019b).

2.2. Data collection and selection criteria

The disdrometer monitored 544 rainy days in the period June 2006 – April 2014 and 50 rainy days in the period October 2016- January 2017 at the Palermo experimental site, and 79 rainy days at the El Teularet experimental site in the period July 2015 – May 2016.

For each rainfall recording minute, the DSDs for which the rainfall intensity was greater than 0.5 mm/h and the measured diameter classes were at least 20 were considered (Carollo et al., 2016; Carollo et al., 2018; Serio et al., 2019a). This choice enables to exclude both rainfall having low erosive power ($I < 0.5$ mm/h) and DSDs having a small simple size (DSD constituted by a number of diameter class less than 20).

Therefore, the dataset considered in this investigation is constituted by 47,860 DSDs, recorded in each rainy minute.

2.3. Fitting and statistical analysis of Weibull and Ulbrich distributions

For the Weibull distribution the probability $P(D)$ that the raindrop diameter is less than D can be calculated, integrating Eq. (2), by the following relationship:

$$P(D) = 1 - e^{-\left(\frac{D}{\sigma}\right)^{\eta}} \quad (3)$$

Eq. (3) underlines that the probability $P(D)$ only depends on σ and η parameters. The mean $m(D)$, the standard deviation $s(D)$, and the median diameter D_{50} of the Weibull distribution are related to the σ and η parameters, as follows:

$$m(D) = \frac{\sigma}{\eta}\Gamma\left(\frac{1}{\eta}\right) \quad (4)$$

$$s(D) = \frac{\sigma}{\eta}\left[2\eta\Gamma\left(\frac{2}{\eta}\right) - \Gamma^2\left(\frac{1}{\eta}\right)\right]^{0.5} \quad (5)$$

$$D_{50} = \sigma(log2)^{\frac{1}{\eta}} \quad (6)$$

being Γ the Gamma function and log the decimal logarithm.

The two distribution parameters, σ and η, of the Weibull distribution (Eq. (2)), were estimated using the Momentum Method (MM) setting the values of D_{50} and D_0, calculated by Eqs. (6) and (19), presented in 3.1 section, equal to the measured ones.

Instead, to employ the Maximum Likelihood method (ML) for estimating Weibull parameters, at first the logarithm function was applied to Eq. (3) for obtaining a linear relationship as:

$$\ln\left[\ln\frac{1}{1-P(D)}\right] = \eta\left[\ln(D) + \ln\left(\frac{1}{\sigma}\right)\right] \quad (7)$$

being Ln the natural logarithm. Eq. (7), been a linear function, allows for estimating the Weibull parameters, σ and η, easy using the Ordinary Last Squared method (Aydi and Alduais, 2022). In this paper, the latter will not be considered as parameter estimate method.

Concerning the gamma distribution, named Ulbrich distribution, the probability $P(D)$ that the raindrop diameter is less than or equal to D can be calculated by as:

$$P(D) = \frac{\Lambda^{4+\mu}}{\Gamma(\mu+1)}\int_0^D D^{\mu} exp(-\Lambda D)dD \quad (8)$$

where Γ is the gamma function. The median raindrop diameter, D_{50}, and the median volume drop diameter, D_0, can be calculated as a function of two parameters, μ and Λ, as:

$$D_{50} = \frac{0.67+\mu}{\Lambda} \quad (9)$$

$$D_0 = \frac{3.67+\mu}{\Lambda} \quad (10)$$

Considering the Ulbrich distribution, Carollo and Ferro (2015) and Carollo et al. (2018) theoretically deduced the following relationships to estimate kinetic power, P_n, and rainfall momentum M:

$$P_n = 10^{-6}\frac{9.5^2}{7.2}\rho\,\Lambda^{4+\mu}\left[\frac{1}{\Lambda^{4+\mu}} - \frac{2}{(6+\Lambda)^{4+\mu}} + \frac{1}{(12+\Lambda)^{4+\mu}}\right]I \quad (11)$$

$$M = 2.64\,10^{-6}\left[1 - \frac{\Lambda^{4+\mu}}{(6+\Lambda)^{4+\mu}}\right]I \quad (12)$$

where ρ is the water density (kg m^{-3}). Eq. (11) and (12) suggest that rainfall kinetic power and momentum are function of the rainfall intensity and μ and Λ parameters of the DSD.

To verify and thus to quantify the reliability of these theoretical distributions to reproduce the DSDs and the energetic characteristics of the precipitation, the following statistic indices have been considered. In particular, the values of the mean relative error (MRE) (%) and the mean absolute error (MAE) (%), are calculated as follows:

$$\text{MRE} = \frac{100}{N_{DSD}}\sum_{i=0}^{N_{DSD}}\left(\frac{x_{calculated} - x_{measured}}{x_{measured}}\right) \quad (13)$$

$$\text{MAE} = \frac{100}{N_{DSD}}\sum_{i=0}^{N_{DSD}}\left|\frac{x_{calculated} - x_{measured}}{x_{measured}}\right| \quad (14)$$

in which $x_{calculated}$ and $x_{measured}$ are the generical name of the calculated and measured considered variables, respectively. Moreover, to evaluate the reliability of Eqs. (3) and (8) to reproduce the DSDs detected at Palermo and El Teularet experimental site, the coefficient of determination, R^2, is calculated as:

$$R^2 = 1 - \frac{\sum \left(P_{(D)i} - P_{(D)}\right)^2}{\sum \left(P_{(D)i} - P_{(D)mean}\right)^2} \tag{15}$$

where $P_{(D)i}$ is the measured probability that the raindrop diameter is less than D, $P_{(D)}$ is the probability calculated by Eq. (3) and $P_{(D)mean}$ is the mean value of the $P_{(D)i}$.

In conclusion, the mean relative error (*MRE*) and mean absolute error (*MAE*) allow for estimating the accuracy of the theoretical relationships proposed to estimate the rainfall kinetic power and momentum while the coefficient of determination, R^2, is used to quantify the difference between the predicted DSD using Weibull distribution and the actual measured value. These statistics helps to evaluate the accuracy of the model and determine its feasibility in practical applications.

3. Results and discussion

3.1. Testing of the reliability of the Weibull distribution in the Mediterranean area

To test the suitability of the Weibull distribution to reproduce the measured DSDs, the raindrop size distributions detected at Palermo and El Teularet have been considered.

Considering that the integral function, $F(D)$, of the Weibull distribution (Eq. (2)) is given by

$$F(D) = N_0\left(1 - exp\left[-\left(\frac{D}{\sigma}\right)^{\eta}\right]\right) \tag{16}$$

the total number of droplets, N, can be calculated as follows

$$N = \int_0^{\infty} N(D)dD = \int_0^{\infty} N_0\,\frac{\eta}{\sigma}\left(\frac{D}{\sigma}\right)^{\eta-1} exp\left[-\left(\frac{D}{\sigma}\right)^{\eta}\right]dD = N_0 \tag{17}$$

Eq. (17) demonstrates that, in contrast with Sekine and Lind (1982), N_0 is not a constant parameter but it has a physical meaning as is equal to the total number of the raindrops that reach the unit soil surface in the unit time.

Considering that the raindrop volume distribution, $Vol(D)$, is calculated by the following relationship:

$$Vol(D) = \frac{\pi}{6}(D)^3 N(D)dD \tag{18}$$

Substituting Eq. (2) in Eq. (18) and considering that the median volume diameter, D_0, is the median diameter of the raindrop volume distribution $Vol(D)$, the following relationship is deduced:

$$D_0 = \sigma\left(\frac{3}{\eta} + 0.67\right)^{\frac{1}{\eta}} \tag{19}$$

Eq. (19) highlights that D_0 is only a function of the σ and η parameters of the Weibull distribution.

The Weibull distribution (Eq. (2)) was fitted to the 47,860 considered DSDs. The two distribution parameters, σ and η, were estimated using the Momentum Method (MM) as described in 2.3 section.

Fig. 3 shows, as an example, for different rainfall intensity values, the fits of Eq. (3) to DSDs detected at Palermo and El Teularet. In particular, this figure highlights that the MM gives similar accuracy for reproducing the DSDs in both sites, registering a mean value of R^2, calculated by Eq. (15), equal to 0.9525 (Palermo) and 0.9615 (El Teularet). To assess the influence of rainfall intensity on the reliability of the Weibull distribution to reproduce the DSDs, for each experimental site the raindrop size

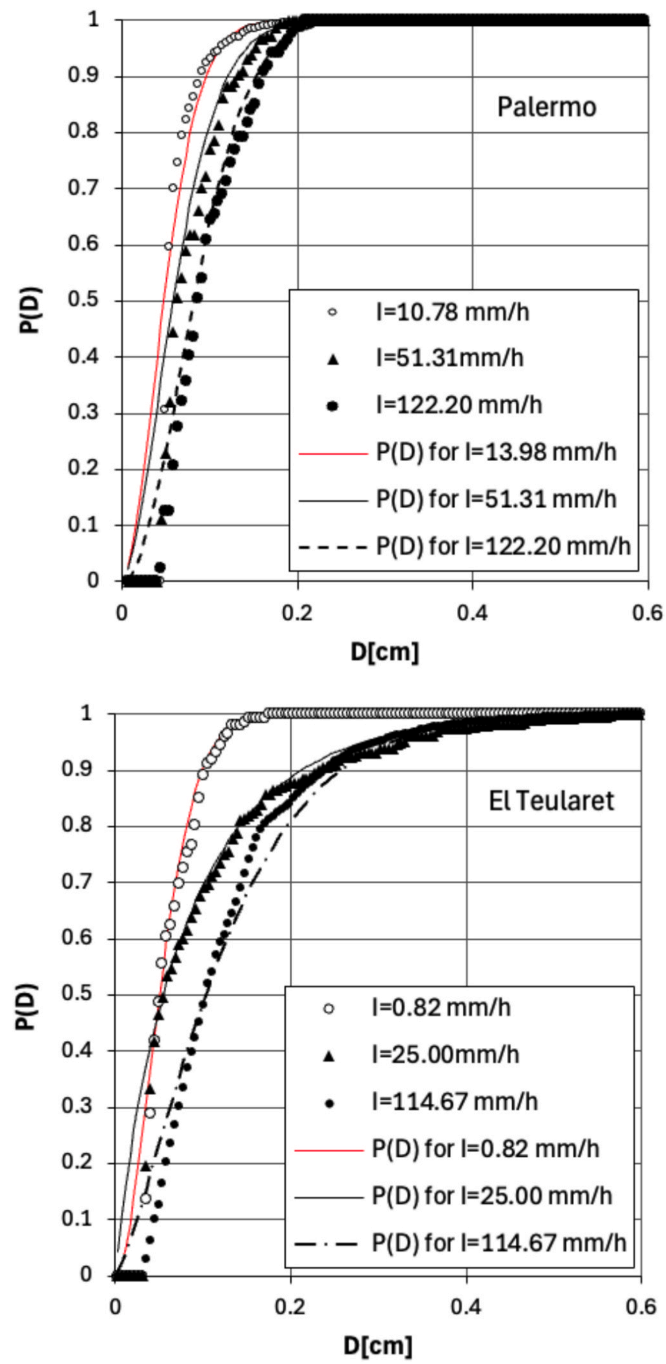

Fig. 3. Examples of fitting of Weibull's distribution at Palermo and El Teularet experimental sites.

distributions have been aggregated into rainfall intensity classes having an amplitude of 5 mm/h. For each class the R^2 and I values have been calculated as the mean value of the R^2 (*mean* R^2) and I (I_{mean}) of the DSDs falling in each class of I. For each experimental site, Fig. 4 shows the comparison between *mean* R^2 versus I_{mean}. Fig. 4 highlights, in agreement with Alonge and Afullo (2012), a decreasing trend of *mean* R^2 with I_{mean}, until a threshold value of I_{mean} equal to 40 mm/h, after which no appreciable trend of the *mean* R^2 with I_{mean} has been observed. For both sites the decreasing accuracy of the fit, and thus of the Weibull parameters estimates, with the increase of the mean value of rainfall intensity could be due to the short sample size of the rainfall intensity classes (Table 1), making the mean value of the R^2 less robust. For each experimental site (Palermo, El-Teluaret), the single DSDs with R^2 less

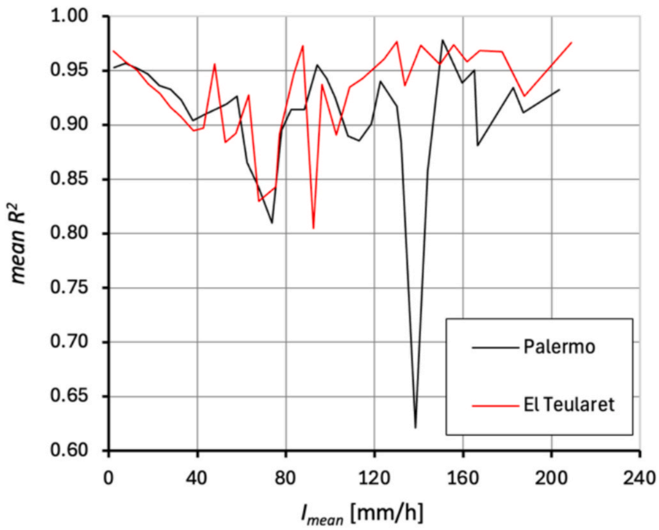

Fig. 4. Relationship between the *mean* R^2 and I_{mean}, for each experimental site.

than 0.8 and with a rainfall intensity greater than 40 mm/h are listed in Table 2.

The analysis highlights that when the fit is least accurate the number of DSDs that meet the criteria of $R^2 < 0.8$ and rainfall intensity $I > 40$ mm/h at the Palermo and El Teularet sites are 29 and 15, respectively. In terms of proportion, such DSDs account for only 0.07% of all measured distributions at the Palermo site, and 0.27% at the El Teularet site. This indicates that although the fitting performance of the Weibull distribution decreases under high rainfall intensity conditions, it still maintains a high level of reliability overall.

Thus, this analysis demonstrated (i) the reliability of the Weibull distribution to reproduce the measured raindrop size distributions considered in the present investigation; (ii) for $I_{mean} > 40$ mm/h a decreasing trend of *mean* R^2 with I_{mean} is observed, which may be influenced by the limited sample size, and this trend is independent of the considered experimental site.

For each experimental site, Fig. 5 shows the relationship between the two parameters estimated using MM method highlighting a very weak correlation between σ and η.

Fig. 6 shows, the comparison between the pairs (σ, I) and (η; I) referred to Palermo and El Teularet. This analysis demonstrated that, the pairs (σ; I) and (η; I) are overlapped and resulted to be poorly correlated with rainfall intensity. Therefore, since for a fixed rainfall intensity DSDs having different values of shape and scale parameters occurred, I could not be considered a variable enabling to synthesize rainfall characteristics. This finding is inconsistent with the previous study of Sekine and Lind (1982), which suggested that the parameters of the Weibull

Table 2
Number of DSDs, for each experimental site, characterized by given ranges of R^2.

		MM		
Experimental site	*DSDs tot.*	*DSDs with* $R^2 > 0.8$	*DSDs with* $R^2 < 0.8$	*DSDs with* $R^2 < 0.8$ *and* $I > 40$ *mm/h*
Palermo	42,279	42,048	231	29
El Teularet	5581	5535	46	15

Table 1
Mean values of the coefficient of determination arranged for rainfall intensity classes.

Palermo					*El Teulaset*		
Range of I [5 mm/h]		I_{mean} [mm/h]	*Mean*R^2 *(MM)*	*Number of DSDs falling in each I class*	I_{mean} [mm/h]	*Mean*R^2 *(MM)*	*Number of DSDs falling in each I class*
0.50	5.50	2.20	0.953	34,529	2.16	0.968	3764
5.50	10.50	7.35	0.957	4998	7.73	0.958	966
10.50	15.50	12.54	0.953	1347	12.55	0.951	396
15.50	20.50	17.63	0.947	541	17.73	0.938	155
20.50	25.50	22.85	0.936	306	22.96	0.929	99
25.50	30.50	27.79	0.933	148	27.77	0.916	45
30.50	35.50	32.71	0.923	104	32.32	0.908	31
35.50	40.50	37.88	0.904	78	38.15	0.895	28
40.50	45.50	42.92	0.909	59	42.81	0.897	16
45.50	50.50	47.47	0.914	36	47.85	0.956	8
50.50	55.50	52.94	0.919	23	52.58	0.884	9
55.50	60.50	57.84	0.926	20	57.30	0.893	9
60.50	65.50	62.49	0.865	11	63.05	0.928	7
65.50	70.50	67.50	0.844	13	67.58	0.830	3
70.50	75.50	73.57	0.810	5	75.28	0.843	2
75.50	80.50	78.03	0.895	7	77.02	0.891	4
80.50	85.50	82.42	0.914	7	83.56	0.947	4
85.50	90.50	88.27	0.914	6	87.51	0.973	2
90.50	95.50	94.03	0.955	2	92.50	0.805	3
95.50	100.50	98.46	0.943	8	96.18	0.937	2
100.50	105.50	102.33	0.925	4	102.79	0.891	3
105.50	110.50	108.11	0.890	1	108.77	0.935	3
110.50	115.50	113.16	0.886	7	114.38	0.943	4
115.50	120.50	118.51	0.901	2	124.38	0.960	2
120.50	125.50	122.71	0.940	3	130.05	0.977	1
125.50	130.50	129.98	0.917	2	133.65	0.936	2
130.50	135.50	132.11	0.885	1	140.82	0.974	1
135.50	140.50	138.42	0.621	1	149.64	0.956	1
140.50	145.50	144.11	0.858	3	155.74	0.974	1
150.50	155.50	150.66	0.978	1	161.75	0.958	2
155.50	160.50	159.66	0.939	1	167.47	0.968	2
160.50	165.50	165.17	0.950	1	177.68	0.967	2
165.50	170.50	166.65	0.881	1	187.78	0.926	3
180.50	185.50	182.54	0.934	1	208.93	0.976	1
185.50	190.50	187.10	0.911	1			
200.50	205.50	203.33	0.932	1			

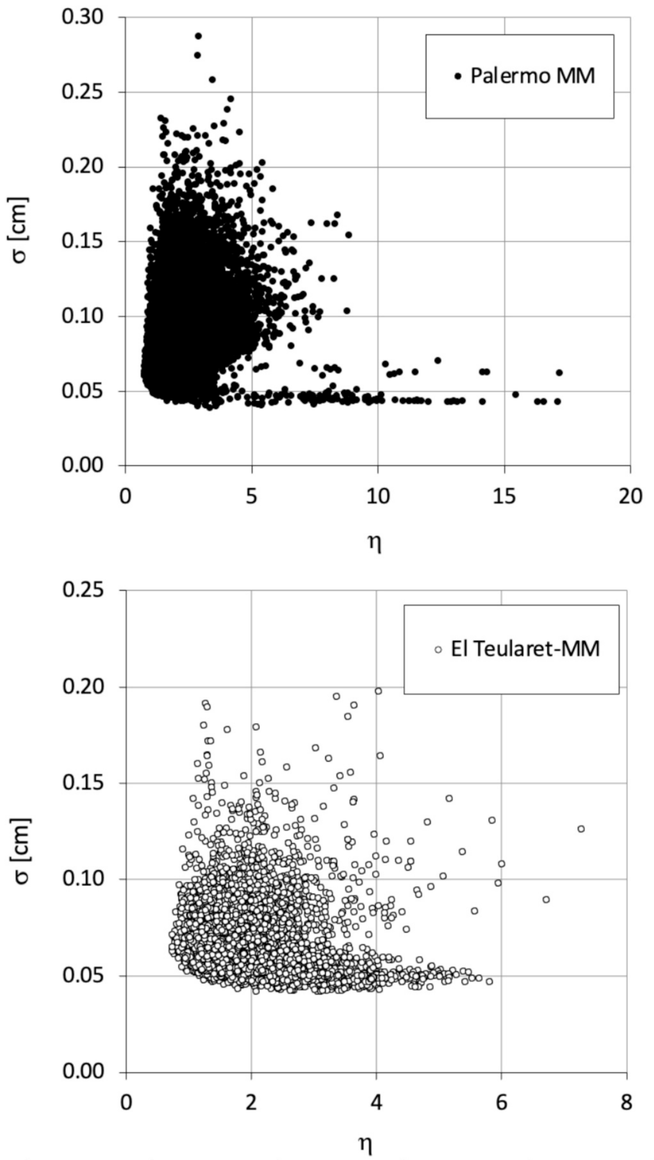

Fig. 5. Plot of the (σ, η) pairs for each experimental site.

distribution are related to rainfall intensity through a power-law relationship. These authors analyzed DSDs detected by Laws and Parsons (1943), Sander (1975), and Wickerts (1982), in geographical sites different from those of the present investigation, and the lack of an analysis supporting the choice of a power low relationship does not allow for the comparison with the results of the present investigation. Nevertheless, Fig. 6 suggests that for Palermo and El Teularet data, the rainfall intensity cannot be used as a variable to comprehensively characterize rainfall features as it is not able to univocally determine the parameters of the Weibull distribution (σ and η).

3.2. A theoretical approach to determine rainfall kinetic power and momentum by Weibull distribution

Considering the Weibull distribution of Eq. (2), equal to the drop size distribution that reaches a unit horizontal area during a unit time, $N(D)$, the following theoretical analysis has been developed.

Rainfall intensity I (mm/h) can be calculated from the following expression (Salles et al., 2002; Carollo and Ferro, 2015):

$$I = 3.6\frac{\pi}{6}\int_0^\infty D^3 N(D)dD \tag{20}$$

in which D is expressed in cm and $N(D)dD$ in m^{-2}s^{-1}. Substituting Eq. (2) in Eq. (20) and solving the integral, Eq. (20) becomes:

$$I = 3.6\frac{\pi}{6}N_0\sigma^3\Gamma\left(\frac{3}{\eta}+1\right) \tag{21}$$

being Γ the gamma function.

Eq. (21) links the DSD parameters to rainfall intensity and allows for calculating the N_0 parameter as a function of I and of the other two Weibull parameters:

$$N_0 = \frac{I}{3.6\frac{\pi}{6}\sigma^3\Gamma\left(\frac{3}{\eta}+1\right)} \tag{22}$$

The kinetic power, P_n (J m^{-2}h^{-1}), is calculated by adding the contribution of each drop that composes precipitation, once their terminal velocity and DSD are known, as:

$$P_n = 10^{-6}\frac{\rho\pi}{12}\int_0^\infty [V(D)]^2 D^3 N(D)dD \tag{23}$$

in which ρ is the water density, equal to 1000 kg/m^3, and $V(D)$ is the raindrop terminal velocity (m/s) of the droplet having a diameter D (cm). Considering the equation proposed by Atlas and Ulbrich (1977) to estimate $V(D)$ as a function of D:

$$V(D) = 17.67D^{0.67} \tag{24}$$

and Eq. (2), Eq. (23) can be rewritten as:

$$P_n = 10^{-6}\frac{\rho\pi}{12}17.67^2 N_0\sigma^{4.34}\Gamma\left(\frac{4.34}{\eta}+1\right) \tag{25}$$

Substituting the N_0 given by Eq. (22), Eq. (25) becomes

$$P_n = 6.273510^{-5}\rho\sigma^{1.34}\frac{\Gamma\left(\frac{4.34}{\eta}\right)}{\Gamma\left(\frac{3}{\eta}\right)}I \tag{26}$$

Eq. (26) enables to calculate P_n when the rainfall intensity I, and the σ and η parameters of the Weibull distribution are known. In other words, the kinetic power per unit volume of rainfall, P_n/I (J/m^2/mm), is only a function of the two parameters of the Weibull distribution. Furthermore, according to Eq. (26), the ratio P_n/I only depends on the intrinsic characteristics of the precipitation, i.e. the scale (σ) and shape (η) parameters of the Weibull raindrop size distribution.

The momentum per unit area and time, M (N m^{-2}), is expressed by the following relationship (Carollo et al., 2018):

$$M = 10^{-6}\frac{\rho\pi}{6}\int_0^\infty V(D)D^3N(D)dD \tag{27}$$

Using the relationship proposed by Atlas and Ulbrich (1977) to estimate the falling velocity and Eq. (2), Eq. (27) can be rewritten as:

$$M = 10^{-6}\frac{\rho}{3.6}17.67\sigma^{0.67}\frac{\Gamma\left(\frac{3.67}{\eta}+1\right)}{\Gamma\left(\frac{3}{\eta}+1\right)}I \tag{28}$$

According to Eq. (28), the rainfall momentum depends on the rainfall intensity and the scale and shape parameters of the Weibull distribution.

For each DSD, the measured values of kinetic power, named *measured* P_n, and of rainfall momentum, named *measured* M, were determined by associating each raindrop diameter with the corresponding terminal velocity calculated by Eq. (24). Fig. 7 shows the

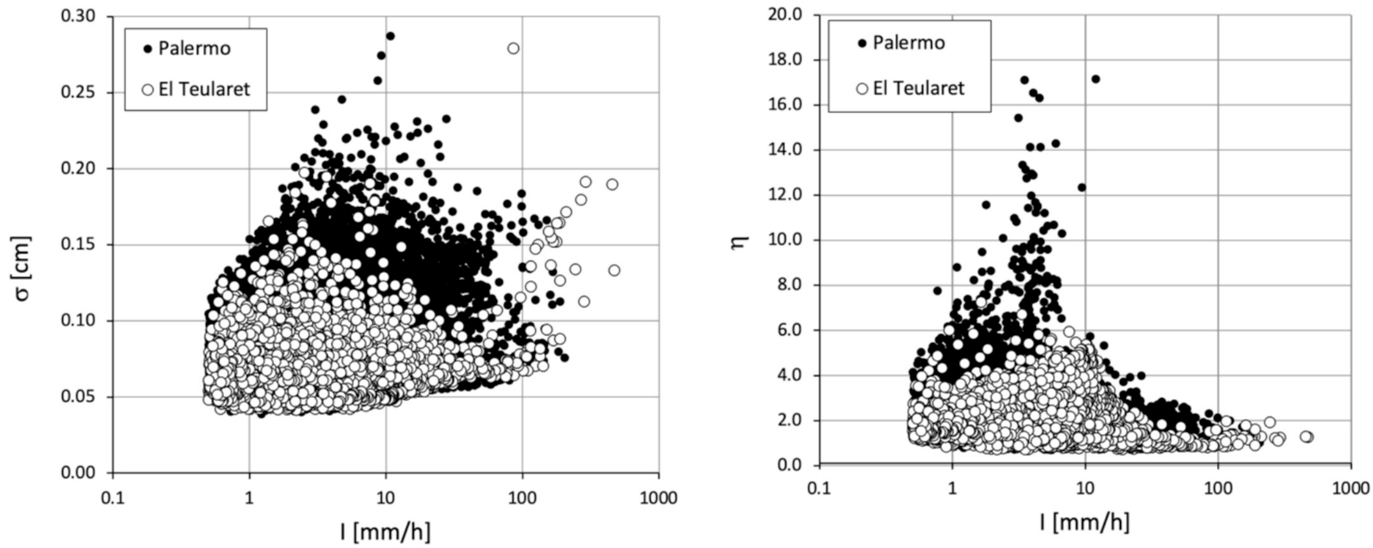

Fig. 6. Relationship between σ and *η* parameters versus rainfall intensity for each experimental site.

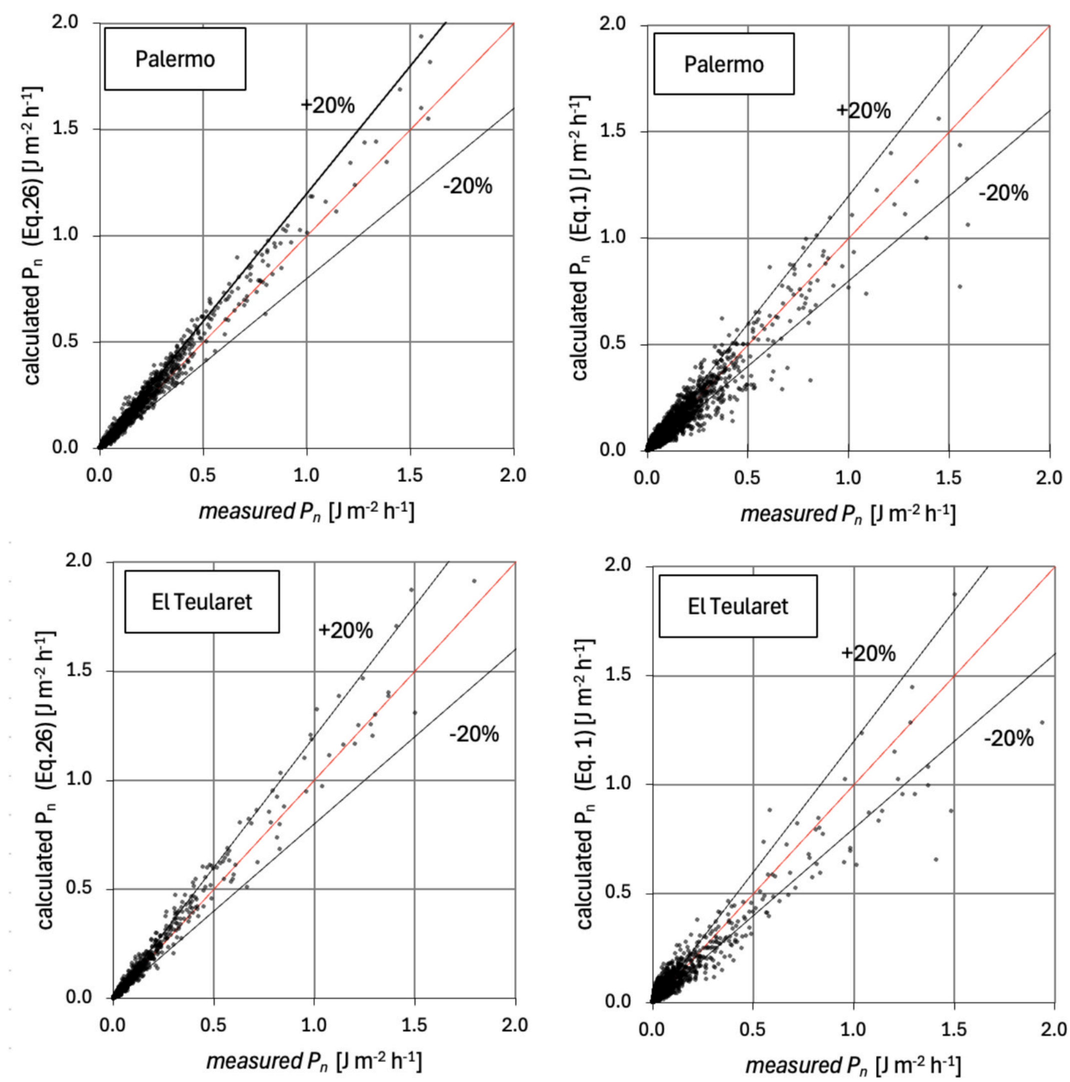

Fig. 7. Comparison between the measured values of P_n and those calculated by Eq. (26) and Eq. (1) by Wischmeier and Smith (1978).

comparison between the *measured* P_n values and those calculated by Eq. (26), named *calculated* P_n, considering MM to estimate σ and η. Despite the dispersion of the points around the line of perfect agreement, the analysis confirms the reliability of Eq. (26) to estimate P_n at Palermo and El Teularet, although a slight underestimation of the rainfall kinetic power is detected (Table 3).

The reliability of Eq. (1) to reproduce the rainfall kinetic power by rainfall intensity was also tested. The comparison between the *measured* P_n values and those calculated by Eq. (1) (Fig. 7) confirms, in agreement with Carollo et al. (2023), that for both dataset Eq. (1) allows for overestimating the P_n values, producing a MRE equal to 31.10% and 68.14% for Palermo and El Teularet site, respectively. In addition, the low percentage of measurements with absolute errors (AE) less than 20%, that resulted to be equal to 24.23% for El Teularet and 36.00% for Palermo (Table 3), suggests the limited accuracy of Eq. (1) to characterize rainfall erosivity in Mediterranean environment and confirmed its site-specificity. Eq. (1) is an empirical relation, whose mathematical form derives from the interpolation of data. Thus, it requires both to be calibrated, and this type of relationship could also be unsuitable for the considered data. On the other hand, Eq. (26) was deduced theoretically and requires the estimation of the two parameters of Weibull distribution using measured DSD. These results also confirm that rainfall intensity is not able synthesize rainfall erosivity characteristics (Serio et al., 2019a, b).

Moreover, the new proposed relationship (Eq. (26)), that considered P_n as function of the rainfall intensity and of the two parameters of the Weibull distribution, gives a more reliable characterization of rainfall kinetic energy for the investigated experimental sites.

For both datasets, the comparison between the *measured* M values and those calculated by Eq. (26), named *calculated* M (N m^{-2}), considering MM to estimate σ and η, is reported in Fig. 8. The analysis confirms the reliability of Eq. (28) to estimate M at Palermo and El Teularet, although a weak underestimation the rainfall momentum (Table 3). Nevertheless, for both datasets more than 98% for MM of the measurements present an absolute error less than 20% (Table 3). Furthermore, for Palermo DSDs with $I > 40$ mm/h and characterized by AE < 20% occur for a percentage greater than 79% and equal to 99% respectively, for P_n and M (Table 4). For El Teularet this percentage is greater than 68% for P_n, while for M estimate, all data with $I > 40$ mm/h present an Absolute Error less than 20% (Table 4).

These results confirm that, to calculate the rainfall kinetic power and the rainfall momentum is more important to adequately estimate D_{50} and D_0 than to reproduce the entire DSD, since that these two statistics allowed to know the shape and the scale parameters of the Weibull distribution. This result can be probably justified because the use of the MM method involves the coincidence of the measured values of D_{50} and D_0 with those calculated by the Weibull distribution. Therefore, in agreement with previous studies (Carollo et al., 2016b; Carollo et al., 2018; Serio et al. 2019a, b) D_{50} and D_0 represent two statistics of the DSDs that enable to synthesize the raindrop size distribution and to characterize energetically the precipitation.

Moreover, in agreement with Carollo et al. (2018) and Serio et al. (2019a), these findings also confirm that the rainfall kinetic power and rainfall momentum are variables able to represent the aggressiveness of precipitation in Mediterranean environments. Nevertheless, for both sites, the measurements highlight that the best estimates are obtained considering the rainfall momentum. This result is consistent with Carollo et al. (2018) that, testing P_n and M relationships theoretically

Table 3
Reliability of Eqs. (1), (26) to estimate P_n and (28) to M estimate at Palermo and El Teularet sites.

	Palermo			El Teularet		
	P_n (J m^{-2}h^{-1})		M (N m^{-2})	P_n (J m^{-2}h^{-1})		M (N m^{-2})
	MM	*Eq. (1)*	*MM*	*MM*	*Eq. (1)*	*MM*
MRE (%)	−3.09	31.10	−1.05	−4.43	68.14	−1.76
MAE (%)	8.83	38.93	3.83	12.41	78.54	5.26
Percentage of data with AE < 20%	93.01	36.00	99.25	80.70	24.23	98.16

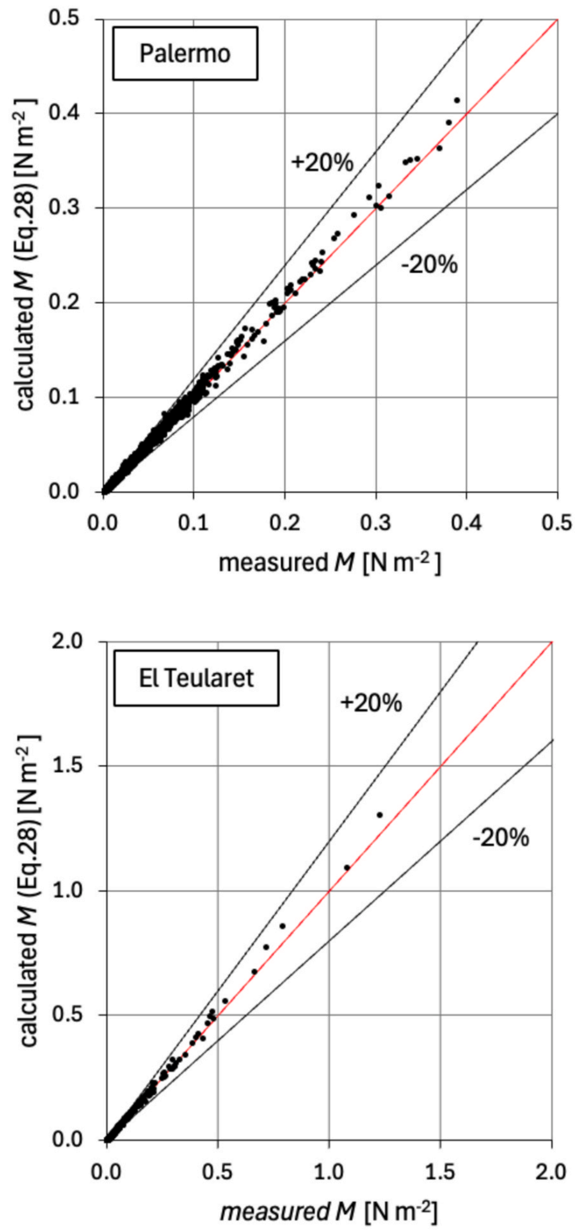

Fig. 8. Comparison between the measured values of M and those calculated by Eq. (28).

Table 4
Number of DSDs with $I > 40$ *mm/h*, for each experimental site, characterized by a P_n (Eq. (26)) and M (Eq. (28)) *AE* value lower than 20%.

Experimental site	*Palermo*	*El Teularet*
Method	MM	MM
DSDs tot.	42,279 5581	
DSDs with I > 40 mm/h	234	105
Percentage of DSDs with AE (Pn) < 20%	89	78
Percentage of DSDs with AE (M) < 20%	99	100

deduced by the Ulbrich distribution to DSDs, considered also in the present investigation, suggested the opportunity to develop a new rainfall erosivity index that includes the rainfall momentum rather than rainfall kinetic power.

3.3. Sensitivity analysis of P_n/I and M/I to Weibull parameters

To assess how changes in σ parameter affect P_n/I and M/I calculated by Eqs (26) and (28), the following first derivatives were calculated:

$$\frac{d\frac{P_n}{I}}{d\sigma} = c1.34\sigma^{0.34} \tag{29}$$

$$\frac{d\frac{M}{I}}{d\sigma} = c_1 0.67\sigma^{-0.33} \tag{30}$$

where c and c_1 are expressed by the following relationships

$$c = 6.273510^{-5}\rho\frac{\Gamma\left(\frac{4.34}{\eta}\right)}{\Gamma\left(\frac{3}{\eta}\right)} \tag{31}$$

$$c_1 = 10^{-6}\frac{\rho}{3.6}17.67\frac{\Gamma\left(\frac{3.67}{\eta}+1\right)}{\Gamma\left(\frac{3}{\eta}+1\right)} \tag{32}$$

Fig. 9 shows, for a fixed η value (as an example, minimum, maximum, and median of the present investigation), the patterns of $\frac{d\frac{P_n}{I}}{d\sigma}$ and $\frac{d\frac{M}{I}}{d\sigma}$ against σ across its experimental range (0.04–0.30 cm). The former (Fig. 9a) increases as σ increases and assumes higher values for the minimum value of η (0.75). Specifically, in this case $\frac{d\frac{P_n}{I}}{d\sigma}$ varies between 0.40 and 0.78, whereas is less than or equal to 0.071 and 0.0095 for the median (1.93) and the maximum (17.17) value of η, respectively.

The derivative $\frac{d\frac{M}{I}}{d\sigma}$ decreases for increasing σ values and it relation with η mirrors that detected for $\frac{d\frac{P_n}{I}}{d\sigma}$. However, the $\frac{d\frac{M}{I}}{d\sigma}$ values are noticeably lower than $\frac{d\frac{P_n}{I}}{d\sigma}$ ones, since they are less than 0.039, resulting M/I less sensitive to σ than P_n/I (Fig. 9).

To perform the sensitivity analysis of P_n/I and M/I with respect to η, Eqs (26) and (28) were applied by imposing a fixed variation in η (for example $\Delta\eta = \pm 1\%$, $\pm 5\%$ and $\pm$ 10%) and computing the consequent variations in P_n/I, $\Delta P_n/I$ (Fig. 10a) and M/I, $\Delta M/I$ (Fig. 10b). Due to the functional relationships between P_n/I and σ (Eq. (26)), and M/I and σ (Eq. (28)), both $\Delta P_n/I$ and $\Delta M/I$ are independent of σ, and therefore, the results depicted in Fig. 10 are valid for any σ. The sign of $\Delta P_n/I$ and $\Delta M/I$ is opposed to the sign of the variation in η and their magnitude is directly related to that of $\Delta\eta$. Similar patterns are detected for all cases, with a reduction of the variations in P_n/I and M/I for increasing η values within the experimental range. These variations tend to vanish for η approximately equal to 5. Similarly to the sensitivity analysis with respect to σ, this analysis points out that M/I is less sensitive to η than P_n/I.

3.4. A new approach to determine the physical and statistical meaning of the Weibull distribution parameters

Sekine and Lind (1982) stated that the parameters η and σ are, respectively, the shape and the scale parameters of the Weibull distribution. Moreover, the raindrop size distributions detected by Laws and Parsons (1943), Sander (1975), and Wickerts (1982), Sekine and Lind (1982) found that both η and σ parameters are related to the rainfall intensity, according to a power low relationship, but these empirical results are not confirmed in this investigation. Therefore, the following theoretical analysis is presented for understanding the existence of the physical meaning of the Weibull parameters, that, at the best of our knowledge, is not suggested in literature.

As η is the shape parameter of Weibull distribution, it depends on the coefficient of variation of the DSD, CV, equal to the ratio between the standard deviation $s(D)$ and the average $m(D)$ of the diameters of the distribution. Therefore, considering Eq. (5) and (6) the coefficient of variation, CV can be calculated as:

$$CV = \frac{s(D)}{m(D)} = \frac{\left[2\eta\Gamma\left(\frac{2}{\eta}\right) - \Gamma^2\left(\frac{1}{\eta}\right)\right]^{0.5}}{\Gamma\left(\frac{1}{\eta}\right)} \tag{33}$$

according to which, the theoretical CV is only dependent on the η parameter, and thus the latter is the primary factor determining the shape of the DSD.

Fig. 11 highlights that in the investigated experimental range (0.3, 17.17) of η, which includes all the expected values, Eq. (33) is a monotonous decreasing function and can be well approximated by the following relationship:

$$\eta = 1.06CV^{-1.054} \tag{34}$$

From a physical point of view, the variation in CV depends on several climatic variables, such as air density, temperature, and aerodynamic

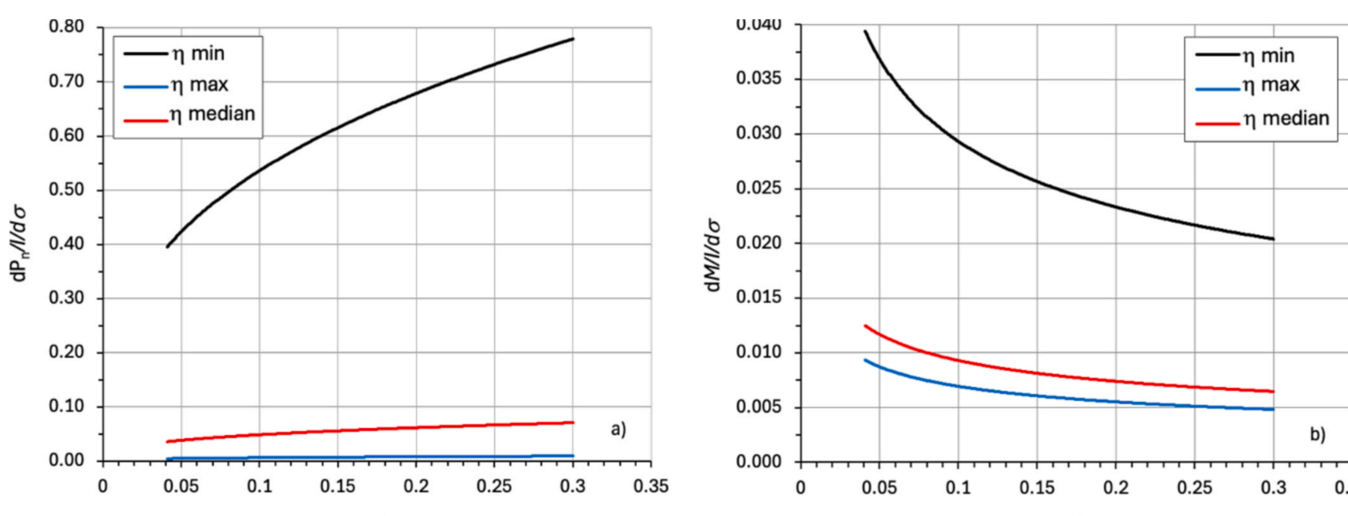

Fig. 9. Patterns of $\frac{d\frac{P_n}{I}}{d\sigma}$ (a) and $\frac{d\frac{M}{I}}{d\sigma}$ (b) against σ for fixed η values.

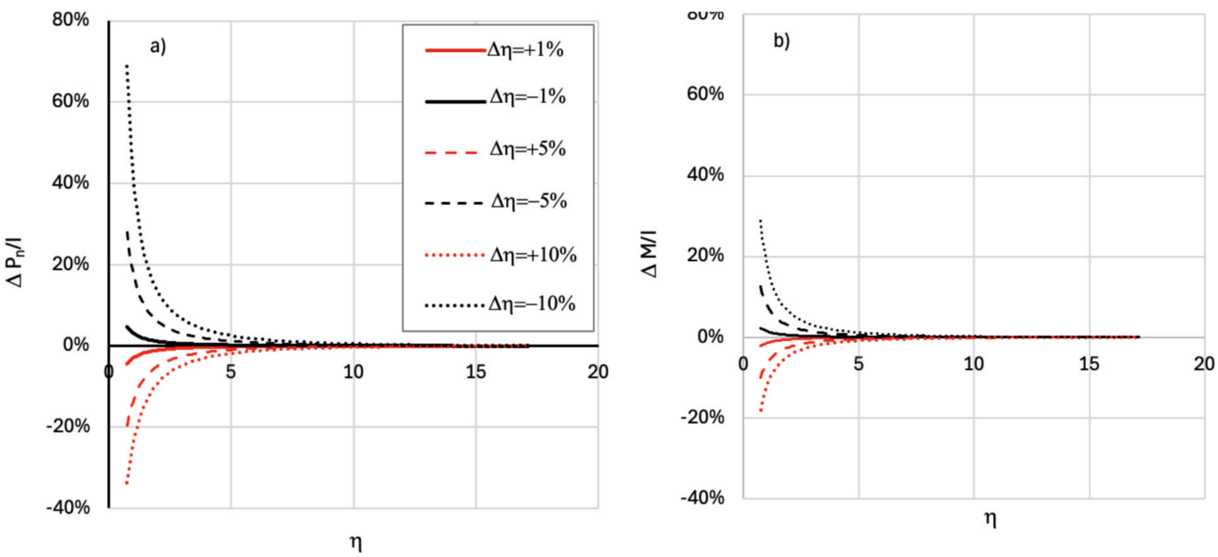

Fig. 10. Sensitivity analysis of P_n/I (a) and M/I (b) with respect to η, for fixed values of the variation in η. $\Delta P_n/I$ and $\Delta M/I$ are the percentage variations of P_n/I and M/I.

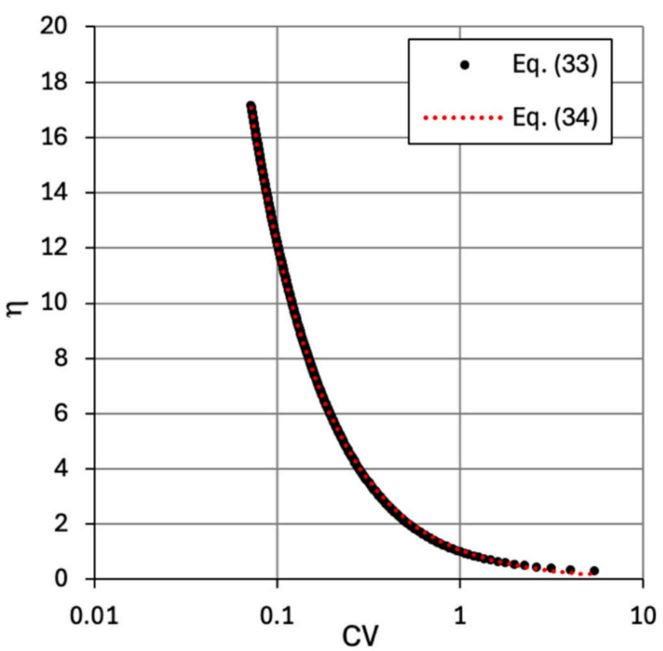

Fig. 11. Plot of the shape parameter η versus the coefficient of variation, CV_W, of the raindrop diameter calculated using the Weibull distribution.

drag. According to Villermaux and Bossa (2009), the latter, acting in concert with raindrop surface tension, is the primary driver for the fragmentation of large single drops into smaller droplets, determining, thus, the shape of the DSD.

Therefore, considering Eq. (26) and Eq. (28), and knowing the values of η by Eq. (34) and of I, the scale parameter, σ, is obtained as:

$$\sigma = kP_n^{\frac{1}{1.34}} \tag{35}$$

and

$$\sigma = k'M^{\frac{1}{0.67}} \tag{36}$$

where k and k' are function of η and I as

$$k = \left(6.273510^{-5}\rho\frac{\Gamma\left(\frac{4.34}{\eta}\right)}{\Gamma\left(\frac{3}{\eta}\right)}I\right)^{-\frac{1}{1.34}} \tag{37}$$

$$k' = \left(10^{-6}\frac{\rho}{3.6}17.67\frac{\Gamma\left(\frac{3.67}{\eta}+1\right)}{\Gamma\left(\frac{3}{\eta}+1\right)}I\right)^{-\frac{1}{0.67}} \tag{38}$$

This analysis leads us to demonstrate that, based on the modalities with which the precipitation occurs (η), a direct relationship exists between the scale parameter (σ) and both the rainfall kinetic power (P_n) (Eq. (35)) and momentum (M) (Eq. (36)). Consequently, this establishes a link between the precipitation's energetic characteristics and the Weibull's scale parameter, conferring upon it a physical significance beyond the statistical one. Specifically, an increase in the value of σ parameter corresponds to a rise in the number of drops with larger diameters within the DSD, which results in a concomitant increase in the values of P_n and M at the soil surface.

3.5. Reliability of Weibull and Ulbrich distributions for estimating the energetic characteristics of rainfall

At first, the Ulbrich (Eq. (8)) distribution was fitted to each DSDs detected at Palermo and El Teularet experimental sites, and the parameters were estimated using the Momentum Method (MM), setting the values of D_{50} and D_0, calculated by Eqs. (9) and (10), equal to the measured values.

To evaluate the reliability of Eq. (8) to reproduce the DSDs detected at Palermo and El Teularet experimental site, for each DSD, the coefficient of determination, R^2, was calculated by Eq. (15).

The comparison between the fittings of the two distributions highlights that the Weibull distribution resulted as reliable as the Ulbrich one to reproduce the DSDs at Palermo and El Teularet sites, registering no significative differences between the performances corresponding to the two experimental sites (Table 5). Indeed, the percentage of DSDs with a R^2 greater than 0.8 is equal to 99.5% and 99.3% for Weibull and Ulbrich distribution, respectively, for Palermo dataset and a R^2 value of about 92.2%, equal for both distributions, is registered for El Teularet experimental site (Table 5). In other words, these results confirm the same

Table 5
Percentage of DSDs, for each distribution and experimental site, characterized by given ranges of R^2.

	DSDs tot.	*Ulbrich distribution*			*Weibull distribution*		
		DSDs with $R^2 > 0.8$	DSDs with $R^2 < 0.8$	DSDs with $R^2 < 0.8$ and $I > 40$ mm/h	DSDs with $R^2 > 0.8$	DSDs with $R^2 < 0.8$	DSDs with $R^2 < 0.8$ and $I > 40$ mm/h
Palermo	42,279	99.3%	0.7%	0.19%	99.5%	0.5%	0.1%
El Teularet	5581	92.2%	7.8%	0.5%	99.2%	0.8%	0.3%

capability of the two distributions to describe more 47,800 measured DSDs considered in the present investigation.

Figs. 12 and 13 show for both datasets the comparison between the measured P_n values and those calculated by Eq. (26) and Eq. (11) (Fig. 12), and between the measured M values and those calculated by Eq. (28) and Eq. (12) (Fig. 13). The analysis suggests that for both datasets, slight underestimations of P_n and M are generally observed considering Eqs. (26) and (28), and a systematic slight overestimation of P_n and M by Eqs. (11) and (12) (Table 6). However, both distributions provide good estimations of P_n and M for $P_n > 0.6$ J m^{-2}h^{-1} and $M > 0.1$ N m^{-2}, that are the most interesting for soil erosion research, even if in this investigation they are very few (Table 6). Nevertheless, Fig. 13 and Table 6 highlighted that both theoretical distributions have similar capability to estimate M since more than 97.80% of DSDs have an absolute error value less than 20%.

Therefore, taking into account the degree of fitting of the theoretical laws to the measured *DSDs* and the reliability of Eq. (28) and Eq. (12) to M estimate, this analysis suggests that the accuracy and the predictive capabilities of the Ulbrich and Weibull distributions are essentially similar for the investigated datasets.

Nevertheless, the Weibull distribution could be preferred both for its capability to P_n and M estimate, and as the parameters of the distribution have also a physical meaning. This allows us to state that there is a direct link between the scale parameter of the distribution, σ, and the energetic characteristics of the precipitation. In other words, the use of the Weibull distribution allowed us to analytically demonstrate that P_n and M depend not only on the intensity of precipitation but also on the disdrometric characteristics of the rainfall reaching the soil.

4. Conclusions

Rainfall erosivity can be assessed by rainfall kinetic power and momentum, which are determined by DSD and raindrop terminal velocity. In this paper, at first, a theoretical analysis was carried out using the Weibull distribution and new relationships to estimate kinetic power and momentum were theoretically deduced.

Through rainfall DSD measurements at two sites in the Mediterranean area, the reliability of these newly proposed theoretical relationships was verified, demonstrating their effectiveness in reflecting the erosive power of rainfall in the Mediterranean environment. Our research indicates that the accurate estimation of the median diameter (D_{50}) and the median volume diameter (D_0) of raindrop size distributions is important. These parameters are integral to capturing the characteristics of rainfall that drive soil erosion processes.

The comparison between the Weibull and the Ulbrich distributions highlighted that, although both distributions yield similar accuracy in terms of DSD fitting, instead for estimating P_n and M, the Weibull model could be favoured as its parameters have also a physical meaning. Moreover, the direct relationship between the scale parameter and the energy characteristics of the precipitation, confirm that P_n and M depend not only on rainfall intensity but also on the properties of the precipitation impacting on the soil surface.

Therefore, the development of a new method and a device able to give a measure of these variables is important to give reliable measures of both P_n and M and thus of the soil loss prediction. Moreover, the results suggest that incorporating rainfall momentum into soil erosion models may offer a more accurate representation than the traditional reliance on kinetic power. However, these conclusions are based on data detected in two sites of the Mediterranean basin and may not be universally applicable to other regions with distinct rainfall characteristics.

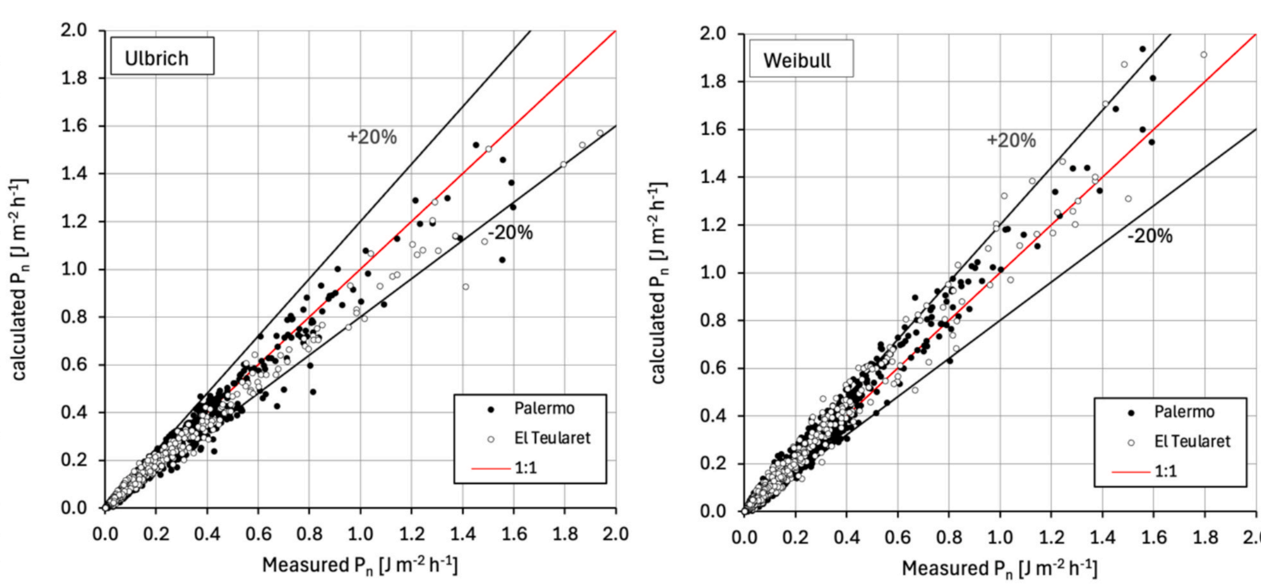

Fig. 12. Comparison between the measured values of P_n and those calculated by Eq. (11), deduced using the Ulbrich distribution, and Eq. (26) deduced using the Weibull distribution.

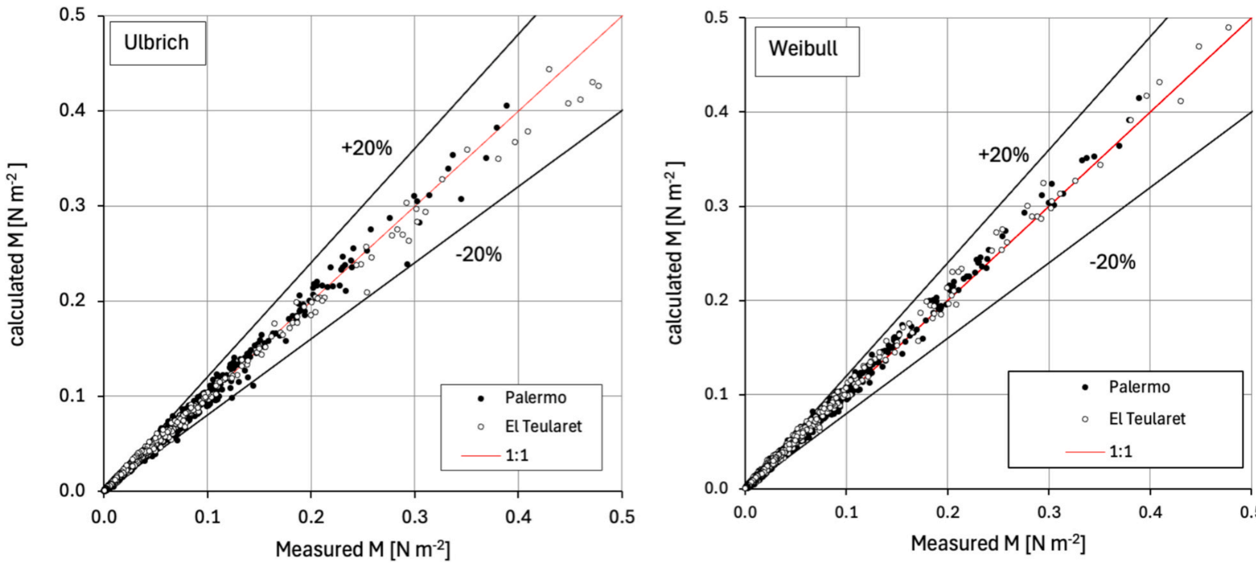

Fig. 13. Comparison between the measured values of M and those calculated by Eq. (12), deduced using the Ulbrich distribution, and Eq. (28) deduced using the Weibull distribution.

Table 6
Reliability of Eqs. (26) and (11) to estimate P_n and Eqs. (28) and (12) to estimate M at Palermo and El Teularet sites.

	Experimental site	Palermo		El Teularet	
	Distribution	Weibull	Ulbrich	Weibull	Ulbrich
P_n	*Number of DSDs*	42,279		5581	
	MRE	−3.14%	19.87%	−4.43%	14.60%
	Percentage of DSDs with AE < 20%	93.1%	43.48%	80.76%	49.22%
M	*MRE*	−1.04%	10.05%	−1.76%	7.48%
	Percentage of DSDs with AE < 20%	99.23%	98.44%	98.23%	97.80%
$P_n > 0.6$ J m^{-2}h^{-1}	*Number of DSDs*	62		50	
	MRE	4.91%	0.65%	3.52%	0.33%
	Percentage of DSDs with AE > 20%	90.3%	85.48%	70.00%	76.00%
$M > 0.1$ N m^{-2}	*Number of DSDs*	137		76	
	MRE	1.00%	0.41%	2.13%	0.48%
	Percentage of DSDs with AE > 20%	100.00%	98.54%	100.00%	100.00%

Further research and validation in diverse environmental contexts are necessary to fully assess the generalizability and applicability of these findings.

CRediT authorship contribution statement

F.G. Carollo: Writing – review & editing, Writing – original draft, Visualization, Validation, Supervision, Methodology, Funding acquisition, Formal analysis, Data curation, Conceptualization. **R. Caruso:** Writing – review & editing, Writing – original draft, Visualization, Validation, Supervision, Methodology, Investigation, Formal analysis, Data curation, Conceptualization. **V. Ferro:** Writing – review & editing, Writing – original draft, Visualization, Validation, Supervision, Methodology, Investigation, Formal analysis, Data curation, Conceptualization. **M.A. Serio:** Writing – review & editing, Writing – original draft, Visualization, Validation, Supervision, Methodology, Investigation, Formal analysis, Data curation, Conceptualization.

Declaration of competing interest

The authors declare that they have no known competing financial interests or personal relationships that could have appeared to influence the work reported in this paper.

Acknowledgments

All authors set up the research, analyzed and interpreted the results, and contributed to write the paper.

This research is funded by “SiciliAn MicronanOTecH Research And Innovation CEnter ”SAMOTHRACE“ (MUR, PNRR-M4C2, ECS_00000022), spoke 3 - Università degli Studi di Palermo ”S2-COMMs - Micro and Nanotechnologies for Smart & Sustainable Communities“.

The DSD measurements at El Teularet were carried out during the stay of Dr. Maria Angela Serio at

the University of Valencia under the supervision of Professor Artemi Cerdà.

Data availability

Data will be made available on request.

References

Abas, N., Daud, Z.M., Yusof, F., 2014. A comparative study of mixed exponential and Weibull distributions in a stochastic model replicating a tropical rainfall process. Theor. Appl. Climatol. 118 (3), 597–607. https://doi.org/10.1007/s00704-013-1060-4.

Ackerman, B., 1967. The nature of the meteorological fluctuations in clouds. J. Appl. Meteor. 6, 61–71. https://doi.org/10.1175/1520-0450(1967)006<0061:TNOTMF>2.0.CO;2.

Alonge, A.A., Afullo, T.J.O., 2012. Seasonal analysis and prediction of rainfall effects in Eastern South Africa at microwave frequencies. Progr. Electromagn. Res. b. 40, 279–303. https://doi.org/10.2528/PIERB12020305.

Angulo-Martínez, M., Beguería, S., Kyselý, J., 2016. Use of disdrometer data to evaluate the relationship of rainfall kinetic energy and intensity (KE-I). Sci. Total Environ. 568, 83–94. https://doi.org/10.1016/j.scitotenv.2016.05.223.

Assouline, S., Mualem, Y., 1989. Similarity of regional rainfall. a dimensionless model of drop size distribution. Trans. Am. Soc. Agric. Eng. 32 (4), 1216–1222. https://doi.org/10.13031/2013.31137.

Assouline, S., 2009. Drop size distributions and kinetic energy rates in variable intensity rainfall. Water Resour. Res. 45, 1–7. https://doi.org/10.1029/2009WR007927.

Assouline, S., 2020. On the relationships between radar reflectivity and rainfall rate and kinetic energy resulting from a Weibull drop size distribution. Water Resour. Res. 56 (10), e2020WR028156. https://doi.org/10.1029/2020WR028156.

Atlas, D., Ulbrich, C.W., 1977. Path and Area-Integrated Rainfall Measurement by Microwave Attenuation in the 1-3 cm Band. J. Appl. Meteorol. Climatol. 16, 1322–1331. https://doi.org/10.1175/1520-0450(1977)016<1322:PAAIRM>2.0.CO;2.

Aydi, W., Alduais, F.S.F., 2022. Estimating Weibull Parameters using Least Squares and Multilayer Perceptron vs. Bayes estimation. Comput. Mater. Contin. 71, 4033–4050. https://doi.org/10.32604/cmc.2022.023119.

Bagarello, V. and Ferro, V., 1998. Calibrating storage tanks for soil erosion measurement from plots. Earth Surf. Process. Landf.: J. Br. Geomorphol. Gr. 23 (13), 1151–1170. https://doi.org/10.1002/(SICI)1096-9837(199812)23:13<1151::AID-ESP929>3.0.CO;2-7.

Bagarello, V., Ferro, V., Pampalone, V., 2013. A new expression of the slope length factor to apply USLE-MM at Sparacia experimental area (Southern Italy). Catena 102, 21–26. https://doi.org/10.1016/j.catena.2011.06.008.

Baumgardner, D., Baker, B., Weaver, K., 1993. A technique for the measurement of cloud structure on centimeter scales. J. Atmos. Oceanic Tech. 10, 557–563. https://doi.org/10.1175/1520-0426(1993)010<0557:ATFTMO>2.0.CO;2.

Bringi, V.N., Chandrasekar, V., Hubbert, J., Gorgucci, E., Randeu, W.L., Schoenhuber, M., 2003. Raindrop size distribution in different climatic regimes from disdrometer and dual-polarized radar analysis. J. Atmos. Sci. 60 (2), 354–365. https://doi.org/10.1175/1520-0469(2003)060<0354:RSDIDC>2.0.CO;2.

Carollo, F.G., Ferro, V., 2015. Modeling Rainfall Erosivity by measured Drop-size Distributions. C4014006-1-7 J. Hydrol. Eng. 20. https://doi.org/10.1061/(ASCE)HE.1943-5584.0001077.

Carollo, F., Ferro, V., Serio, M.A., 2016a. Estimating rainfall erosivity by aggregated drop size distributions. Hydrol. Process. 30, 2119–2128. https://doi.org/10.1002/hyp.10776.

Carollo, F., Ferro, V., Serio, M.A., 2016b. Reliability of rainfall kinetic power- intensity relationships. Hydrol. Process. 31 (6), 1293–1300. https://doi.org/10.1002/hyp.11099.

Carollo, F.G., Ferro, V., Serio, M.A., 2018. Predicting rainfall erosivity by momentum and kinetic energy in Mediterranean environment. J. Hydrol. 560, 173–183. https://doi.org/10.1016/j.jhydrol.2018.03.026.

Carollo, F.G., Nicosia, A., Palmeri, V., Pampalone, V., Serio, M.A., Ferro, V., 2023. Measuring Rainfall Kinetic Power in two Sicilian Experimental areas by Drop-size distribution Data. Land 12 (2), 418. https://doi.org/10.3390/land12020418.

Carter, C.E., Greer, J.D., Braud, H.J., Floyd, J.M., 1974. Raindrop characteristics in South Central United States. Trans. Am. Soc. Agric. Eng. 17, 1033–1037.

Cevasco, A., Diodato, N., Revellino, P., Fiorillo, F., Grelle, G., Guadagno, F.M., 2015. Storminess and geo-hydrological events affecting small coastal basins in a terraced Mediterranean environment. Sci. Total Environ. 532, 208–219. https://doi.org/10.1016/j.scitotenv.2015.06.017.

Cohen, A.C., 1965. Maximum Likelihood Estimation in the Weibull distribution based on complete and on Censored Sample. Technometrics 7, 579–588. https://doi.org/10.1080/00401706.1965.10490300.

Feingold, G., Levin, Z., 1986. The lognormal fit to raindrop spectra from convective clouds in Israel. J. Clim. Appl. Meteorol. 25, 1346–1363. https://www.jstor.org/stable/26182572.

Ferro, V., 2001. Tecniche di misura e monitoraggio dei processi erosivi. Quad. Idr. Mont. 21 (2), 63–128 in Italian.

Falkovich, G., Fouxon, A., Stepanov, M., 2002. Acceleration of rain initiation by turbulence. Nature 419, 151–154.

García-Orenes, F., Cerdà, A., Mataix-Solera, J., Guerrero, C., Bodí, M.B., Arcenegui, V., Zornoza, R., Sempere, J.G., 2009. Effects of agricultural management on surface soil properties and soil–water losses in eastern Spain. Soil Tillage Res. 106 (1), 117–123.

Grossklaus, M., Uhlig, K., Hasse, L., 1998. An optical disdrometer for use in high wind speeds. J. Atmos. Oceanic Tech. 15 (4), 1051–1059.

Hudson, N.W., 1965. The influence of rainfall mechanics on soil erosion. Msc Thesis, Cape Town.

Jiang, H., Sano, M., Sekine, M., 1996. Radar reflectivity and rainfall rate relation from Weibull raindrop-size distribution. IEICE Trans. Commun. 79 (6), 797–800.

Jiang, H., Sano, M., Sekine, M., 1997. Weibull raindrop-size distribution and its application to rain attenuation. IEE Proc. Microw. Antennas Propag. 144 (3), 197–200. https://doi.org/10.1049/ip-map:19971193.

Khrgian, A.K.A., Mazin, I.P., Cao, V., 1952. Distribution of drops according to size in cloud. Tr. Tsent. Aerol. Observ. 7, 56.

Kumar, V., Jahangeer, S., 2017. Statistical distribution of rainfall in Uttarakhand, India. Appl. Water Sci. 7 (8), 4765–4776. https://doi.org/10.1007/s13201-017-0586-5.

Laflen, J.M., Moldenhauer, W.C., 2003. Pioneering soil erosion prediction. The USLE Story. World Association of Soil & Water Conservation. Special Publication N.1.

Laws, J.O., Parsons, D.A., 1943. The relation of raindrop size to intensity. Trans. Am. Geophys. Union 24, 452–460. https://doi.org/10.1029/TR024i002p00452.

Lempio, G.E., Bumke, K., Macke, A., 2007. Measurement of solid precipitation with an optical disdrometer. Adv. Geosci. 10, 91–97.

Levin, L.M., 1963. Studies in the physics of roughly dispersed aerosols. U.S. Army Biological Laboratories, Fort Detrick, Frederick, Maryland.

Lim, Y.S., Kim, J.K., Kim, J.W., Park, B.I., Kim, M.S., 2015. Analysis of the relationship between the kinetic energy and intensity of rainfall in Daejeon, Korea. Quat. Int. 384, 107–117. https://doi.org/10.1016/j.quaint.2015.03.021.

Liu, Y., Hallett, J., 1998. On size distributions of cloud droplets growing by condensation: a new conceptual model. J. Atmos. Sci. 55 (4), 527–536. https://doi.org/10.1175/1520-0469(1998)055<0527:OSDOCD>2.0.CO;2.

Marshall, J.S., Palmer, W.M., 1948. The distribution of raindrops with size. J. Atmos. Sci. 5 (4), 165–166. https://doi.org/10.1175/1520-0469(1948)005<0165:TDORWS>2.0.CO;2.

Meshesha, D.T., Tsunekawa, A., Tsubo, M., Haregeweyn, N., Adgo, E., 2014. Drop size distribution and kinetic energy load of rainfall events in the highlands of the Central Rift Valley, Ethiopia. Hydrol. Sci. J. 59, 2203–2215. https://doi.org/10.1080/02626667.2013.865030.

Meshesha, D.T., Tsunekawa, A., Haregeweyn, N., 2019. Influence of raindrop size on rainfall intensity, kinetic energy, and erosivity in a sub-humid tropical area: a case study in the northern highlands of Ethiopia. Theor. Appl. Climatol. 136 (3), 1221–1231. https://doi.org/10.1007/s00704-018-2551-0.

Mualem, Y., Assouline, S., 1989. Modeling soil seal as a nonuniform layer. Water Resour. Res. 25 (10), 2101–2108. https://doi.org/10.1029/WR025i010p02101.

Olivera, S., Heard, C., 2019. Increases in the extreme rainfall events: using the Weibull distribution. Environmetrics 30 (4), e2532. https://doi.org/10.1002/env.2532.

Pampalone, V., Nicosia, A., Palmeri, V., Serio, M.A., Ferro, V., 2023. Rill and interrill soil loss estimations using the USLE-MB equation at the Sparacia Experimental Site (South Italy). Water 15 (13), 2396. https://doi.org/10.3390/w15132396.

Rosewell, C.J., 1986. Rainfall Kinetic Energy in Eastern Australia. J. Clim. Appl. Meteor. 25, 1695–1701. https://doi.org/10.1175/1520-0450(1986)025<1695:RKEIEA>2.0.CO;2.

Salles, C., Poesen, J., Sempere-Torres, D., 2002. Kinetic energy of rain and its functional relationship with intensity. J. Hydrol. 257 (1–4), 256–270. https://doi.org/10.1016/S0022-1694(01)00555-8.

Sander, J., 1975. Rain attenuation of millimeter waves at λ=5.77, 3.3 and 2 mm. IEEE Trans. Antennas Propag. 23 (2), 213–220. https://doi.org/10.1109/TAP.1975.1141059.

Seela, B.K., Janapati, J., Lin, P.L., Wang, P.K., Lee, M.T., 2018. Raindrop size distribution characteristics of summer and winter season rainfall over north Taiwan. J. Geophys. Res.: Atmospheres 123 (20), 11602–11624. https://doi.org/10.1029/2018JD028307.

Sekine, M. Lind, G., 1982. Rain attenuation of centimeter, millimeter and submillimeter radio waves. Proc. 12th Eur. Microw. Conf., Helsinki, Finland. 586-589. https://doi.org/10.1109/EUMA.1982.333124.

Sekine, M., Chen, C.D., Musha, T., 1987. Rain attenuation from log-normal and Weibull rain-drop distributions. IEEE Trans. Antennas Propagat. AP-35(3), 358–359. https://doi.org/10.1109/TAP.1987.1144099.

Sekine, T. Musha and C.D. Chen, 1988. Rain Attenuation from Weibull Raindrop-Size Distribution, Proc. 18th Eur. Microw. Conf., Stockholm, 12-15 September 1988, pp. 423-428. https://doi.org/10.1109/EUMA.1988.333850.

Serio, M.A., Carollo, F.G., Ferro, V., 2019a. A method for evaluating rainfall kinetic power by a characteristic drop diameter. J. Hydrol. 577, 123996. https://doi.org/10.1016/j.jhydrol.2019.123996.

Serio, M.A., Carollo, F.G., Ferro, V., 2019b. Raindrop size distribution and terminal velocity for rainfall erosivity studies. A review. J. Hydrol. 576, 210–228. https://doi.org/10.1016/j.jhydrol.2019.06.040.

Smith, J.A., Hui, E., Steiner, M., Baeck, M.L., Krajewski, W.F., Ntelekos, A.A., 2009. Variability of rainfall rate and raindrop size distributions in heavy rain. Water Resour. Res. 45 (4). https://doi.org/10.1029/2008WR006840.

Sulakvelidze, G.K., 1969. Rainstorms and Hail. Translated from Russian by Israel Program for Scientific Translations. Jerusalem.

Sulakvelidze, G.K., Dadali, Y.A., 1971. Multiwave length radar measurements of precipitation intensity. Radar meteorol., Proc. Third All- Union Conf. (translated from Russian) Israel Progr. Sci. Transl. 32–45 available from NTIS.

Parsons, A.J., Gadian, A.M., 2000. Uncertainty in modelling the detachment of soil by rainfall. Earth Surf. Process. Landf. 25 (7), 723–728.

Tao, D.Q., Nguyen, V.T., Bourque, A., 2002. On selection of probability distributions for representing extreme precipitations in Southern Quebec. Ann Conf Can Soc Civ Eng 1–8.

Tokay, A., Kruger, A., Krajewski, W.F., 2001. Comparison of drop size distribution measurements by impact and optical disdrometers. J. Appl. Meteorol. Climatol. 40 (11), 2083–2097. https://doi.org/10.1175/1520-0450(2001)040<2083:CODSDM>2.0.CO;2.

Uijlenhoet, R., Stricker, J.N.M., 1999. Dependence of rainfall interception on drop size-a comment. J. Hydrol. 217, 157–163. https://doi.org/10.1016/S0022-1694(99)00004-9.

Ulbrich, C.W., 1983. Natural variations in the analytical form of the raindrop size distribution. J. Clim. Appl. Meteorol. 22, 1764–1775. https://www.jstor.org/stable/26181251.

Van Dijk, A.I.J.M., Bruijnzeel, L.A., Rosewell, C.J., 2002. Rainfall intensity–kinetic energy relationships: a critical literature appraisal. J. Hydrol. 261 (1–4), 1–23. https://doi.org/10.1016/S0022-1694(02)00020-3.

Villermaux, E., Bossa, B., 2009. Single-drop fragmentation determines size distribution of raindrops. Nat. Phys. 5 (9), 697–702.

Weibull, W., 1951. A statistical distribution function of wide applicability. J. Appl. Mechanics 293–297.

Waldvogel, A., 1974. The N_0 jump of raindrop spectra. J. Atmos. Sci. 31, 1067–1078. https://doi.org/10.1175/1520-0469(1974)031<1067:TJORS>2.0.CO;2.

Wickerts, S., 1982. Drop size distribution in rain. FOA Report. C20438–E1(E2).

Wischmeier, W.H., 1959. A rainfall erosion index for a Universal Soil loss Equation. Soil Sci. Soc. Am. Proc. 23 (3), 246–249.

Wischmeier, W.H., Smith, D.D., 1978. Predicting Rainfall Erosion Losses: a Guide to Conservation Planning Agricultural Handbook, No. 537. US Department of Agriculture, Washington, DC.

Zhang, G., Vivekanandan, J., Brandes, E.A., Meneghini, R., Kozu, T., 2003. The shape–slope relation in observed gamma raindrop size distributions: statistical error or useful information? J. Atmos. Ocean. Technol. 20 (8), 1106–1119. https://doi.org/10.1175/1520-0426(2003)020<1106:TSRIOG>2.0.CO;2.